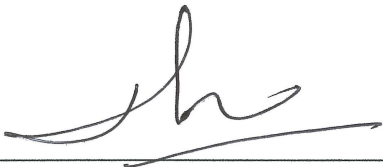


SUPERVISOR'S DECLARATION

We hereby declare that we have checked this thesis and in our opinion, this thesis is adequate in terms of scope and quality for the award of the degree of Master of Science in Mechanical Engineering.



(Supervisor's Signature)

Full Name : MAHADZIR BIN ISHAK @ MUHAMMAD

Position : ASSOCIATE PROFESSOR

Date : 7/7/2017



(Co-supervisor's Signature)

Full Name : FADHLUR RAHMAN BIN MOHD ROMLAY

Position : DOCTOR / SENIOR LECTURER

Date : 7/7/2017



STUDENT'S DECLARATION

I hereby declare that the work in this thesis is based on my original work except for quotations and citations which have been duly acknowledged. I also declare that it has not been previously or concurrently submitted for any other degree at Universiti Malaysia Pahang or any other institutions.

A handwritten signature in black ink, appearing to be 'Muhammad Naquiddin Bin Mat Salleh', is written above a horizontal line.

(Student's Signature)

Full Name : MUHAMMAD NAQUIDDIN BIN MAT SALLEH

ID Number : MMM 14029

Date : 7/7/2017

A STUDY ON DOUBLE FILLET LAP WELDING OF THIN SHEET AZ31B
MAGNESIUM ALLOY BY LOW POWER FIBER LASER

MUHAMMAD NAQUIDDIN BIN MAT SALLEH

Thesis submitted in fulfilment of the requirements
for the award of the degree of
Master of Science

Faculty of Mechanical Engineering
UNIVERSITI MALAYSIA PAHANG

JULY 2017

PERPUSTAKAAN 041017 UNIVERSITI MALAYSIA PAHANG P	
No. Perolehan 119753	No. Panggilan PKM H37
Tarikh 15 SEP 2017	2017 r Thesis

ACKNOWLEDGEMENTS

First and foremost, I would like to express my sincere gratitude to my supervisor, Associate Professor Dr Mahadzir Bin Ishak@Muhammad and my co-supervisor, Dr. Fadhlur Rahman bin Mohd Romlay for his invaluable guidance, ideas, constant encouragement and continuous support in making this research project possible. I am grateful for their consistent support throughout the project with patience and knowledge while allowing me the room to work on my own. I would also like to thank them for the time spent on proofreading and correcting the mistakes in the thesis.

Certainly, not forget the Faculty of Mechanical Engineering, UMP for providing the support and equipment required in the present study. My sincere thanks also go to all my lab mates and members of the technical staffs of Faculty of Mechanical Engineering especially the instructor engineers, Mr Zulkarnain and Mr Azuwar who helped me in many ways especially with the operation of machines and equipment.

Last but not least, I would like to thank my loving parents and my brothers and sister for their continuous support and guidance throughout my master study in Universiti Malaysia Pahang. Without the encouragements from them, I could not possibly afford to pursue this level of study.

ABSTRAK

Tesis ini membentangkan kajian kimpalan laser kepingan nipis AZ31B Magnesium (Mg) aloi menggunakan laser gentian berkuasa rendah. AZ31B dikenali sebagai logam yang lebih ringan berbanding aloi aluminium (Al) dan keluli dengan ketumpatan 1.78 g/cm^3 . AZ31B berketebalan nipis digunakan dalam aplikasi automotif, penerbangan dan bahagian peranti elektronik seperti selongsong komputer dan kepingan nipis di dalam telefon pintar. Kimpalan laser berpotensi sebagai kaedah yang baik untuk pengimpalan AZ31B nipis berbanding dengan kimpalan arka dan kimpalan berkeadaan pepejal di dalam menghasilkan hasil kimpal yang kecil. Kimpalan laser gentian berkuasa rendah dipilih dalam penyelidikan ini dan parameter kimpalan dioptimumkan dengan kaedah sambutan permukaan (RSM) menggunakan kaedah reka bentuk Box-Behnken (BBD) untuk mendapatkan keadaan yang paling sesuai bagi mengimpal AZ31B nipis ini. Kaedah kimpalan laser dengan menggunakan sambungan tindih kambi berganda dipilih kerana ia boleh menghasilkan masukan haba yang rendah bersama kuasa yang tinggi pada ketebalan 0.6 mm disebabkan oleh geometri kimpal sambungan tindih kambi di mana alur difokuskan di hujung kepingan atas. Ia dipilih kerana penggunaan laser yang amat berpengaruh terutama di dalam industri pembuatan. Objektif pertama penyelidikan ini adalah untuk mengoptimumkan parameter kimpalan laser untuk mengimpal sambungan tindih kambi berganda terhadap AZ31B. Objektif kedua ialah untuk menyiasat kaitan antara perubahan mikrostruktur pada sifat-sifat mekanikal untuk sambungan ini. Mengikut reka bentuk eksperimen (DOE) yang dihasilkan oleh BBD, 15 sampel telah dikimpal dan kekuatannya diuji menggunakan ujian kekuatan tegangan ricih. Dari sambutan, model matematik dibina selepas pelaksanaan analisis varians (ANOVA). Membincangkan hubungan antara kekuatan ricih dan mikrostruktur, sampel yang dikimpal kemudian dipotong pada keratan rentas kimpalan yang stabil dan telah dipersiapkan untuk pemerhatian makro dan mikrostruktur. Sampel 9 mempunyai kekuatan ketegangan ricih tertinggi iaitu 62.0 MPa dan beban patah ialah 740 N. Satu model matematik dengan persamaan kuadratik telah dihasilkan untuk menghitung kekuatan tegangan ricih. Untuk pengesahan model matematik, peratusan kesilapan bagi semua sampel adalah kurang daripada 8%. Ia menunjukkan kejituan yang tinggi dan telah diterima. Parameters kimpalan kemudian diteruskan untuk dioptimumkan. Parameter yang dioptimumkan adalah; tenaga denyut (EP): 2.2 J; kelajuan kimpalan (WS): 2.0 mm/s; dan sudut penyinaran (AOI): 2.0° . Peratusan kesilapan bagi sampel yang dioptimumkan ialah 0.79 %. Ujian kekerasan Vickers dilakukan pada kawasan kimpalan untuk sampel dengan tertinggi dan sampel yang telah dioptimumkan untuk tujuan perbandingan. Diperhatikan bahawa kebanyakan sampel yang dikimpal mempunyai pemejalan retak di tengah kawasan kimpalan bagi kumai kimpal kedua dan kecacatan ini menyumbang kepada kekuatan tegangan ricih yang lebih rendah berdasarkan makrograf yang telah diperhatikan. Untuk mikrostruktur, bijian yang halus telah terhasil di zon pelakuran (FZ) berbeza daripada FZ berdekatan dengan garisan peralihan yang mana menghasilkan bijian yang kasar dan sederhana. Sampel yang dioptimumkan telah patah di kawasan peralihan pada kepingan atas, manakala sampel 1 patah pada kimpal diebabkan oleh kecacatan retak. Diperhatikan bahawa patah tersebut adalah rapuh. Sampel yang dioptimum mempunyai 80.5 Mpa kekuatan tegangan ricih dengan daya beban 800 N dimana boleh menggantikan Al dan keluli terutama untuk peranti electronic kerana kekuatan tersebut diterima untuk produk yang nipis.

ABSTRACT

This thesis presents a study on laser welding of thin sheet AZ31B Magnesium (Mg) alloys using low power fiber laser. AZ31B is known as the lighter metal compared to aluminium alloys and steel with the density of 1.78 g/cm^3 . Thin sheet AZ31B finds its application in automotive, aviation and also electronic devices parts such as computer casing and thin plate part in smartphone. In joining thin sheet AZ31B, laser welding is promising the best joining method compared to arc and solid state welding in producing small weldments. A low power fiber laser welding has been chosen in this research work and the welding parameters are optimized by response surface method (RSM) using Box-Behnken design (BBD) method in order to provide the most suitable laser welding condition to weld this thin AZ31B. Welding as thin as 0.6 mm of AZ31B, laser welding by double fillet lap joint configuration is selected as it can produce lower heat input with high power due to the weld geometry of fillet lap joint which beam focused at the edge of upper sheet. It was preferred since the usage of laser was overwhelming especially in manufacturing industries. The first objective of this work is to optimize the laser welding parameters to weld double fillet lap joint on AZ31B. The second objective is to investigate the relation of microstructure changes on mechanical properties of this joint. According to design of experiment (DOE) generated by BBD, 15 samples are welded and their strength were tested using tensile-shear test. From the response, a mathematical model is constructed after the analysis of variance (ANOVA) has been performed. To discuss the relationship between the shear strength and microstructure, welded samples are cut at the stable weld's cross section and are prepared for the macro and microstructure observation. Sample 9 possesses the highest shear strength with 62.0 MPa and fracture load of 740 N. A mathematical model with quadratic equation was produced to calculate the tensile shear strength. For validation of mathematical model, percentage errors for all samples are less than 8 %. It shows a high accuracy of the model and it was accepted. Welding parameters then proceed to be optimized. The optimized parameters were; pulsed energy (EP): 2.2 J; welding speed (WS): 2.0 mm/s; and angle of irradiation (AOI): 2.0° . The percentage error for the optimized sample was 0.79 %. Vickers hardness test was performed at the weld area for sample with highest and optimized parameter sample in order to compare the result. It was observed that most of the welded samples have the solidification crack at the weld centre area of the second weld and this defect contributed to the lower tensile shear strength as observed from macrograph. For microstructure, finer grain produced at the fusion zone (FZ) of upper sheet compared to the FZ near the transition line which produced coarser and medium grain. Optimized sample was fractured at the transition region of upper sheet, meanwhile sample 1 fractured at the weld due to the crack defect. It was observed that the fracture was brittle. The fine grain produced higher hardness values compared to the coarser grain with a value of 77 Hv for the optimized sample. Optimized sample has 80.5 MPa of tensile shear strength and fracture load of 800 N which could be applied in replacing Al and steel especially for the electronic parts since the strength was acceptable for a thin product.

TABLE OF CONTENT

DECLARATION	
TITLE PAGE	
ACKNOWLEDGEMENTS	ii
ABSTRAK	iii
ABSTRACT	iv
TABLE OF CONTENT	v
LIST OF TABLES	ix
LIST OF FIGURES	x
LIST OF SYMBOLS	xiii
LIST OF ABBREVIATIONS	xiv
CHAPTER 1 INTRODUCTION	1
1.1 Research Background	1
1.2 Problem Statement	4
1.3 Research Objectives	6
1.4 Research Scopes	6
1.5 Thesis Outline	7
CHAPTER 2 LITERATURE REVIEW	8
2.1 Introduction	8
2.2 Magnesium Alloys	8

2.3	Thin Sheet AZ31B	12
2.4	Laser Welding	12
2.4.1	Fiber Laser Welding	15
2.4.2	Continuous Wave Mode	19
2.4.3	Pulse Wave Mode	20
2.5	Laser Welding of AZ31B Mg Alloy	23
2.6	Laser Welding Parameters	25
2.6.1	Pulsed Energy	25
2.6.2	Welding Speed	26
2.6.3	Angle of Irradiation	28
2.7	Microstructure Evolution of Welded AZ31B	30
2.8	Design of Experiment (DOE)	32
2.8.1	Response Surface Method (RSM)	34
2.8.2	Box-Behnken Design (BBD)	36
2.8.3	Analysis of Variance (ANOVA)	37
2.8.4	Mathematical Modelling	39
2.8.5	Data Validation	40
2.8.6	Parameters Optimization	40
2.9	Summary	41
 CHAPTER 3 METHODOLOGY		 43
3.1	Introduction	43
3.2	Research Flow	43
3.3	Material Confirmation and Preparation	45
3.3.1	Sample Preparation for Pre-experiment	45
3.3.2	Sample Preparation for Experiment	46

3.4	Apparatus Setup	46
3.5	Preliminary Experiment	48
3.6	Design of Experiment (DOE)	48
3.7	Tensile-shear Test	49
3.8	Sample Preparation (Macro and Microstructure)	50
3.8.1	Macrostructure Evaluation	51
3.8.2	Microstructure Analysis	51
3.8.3	Grain Size Measurement	52
3.9	Microhardness Test	52
CHAPTER 4 RESULTS AND DISCUSSION		54
4.1	Introduction	54
4.2	Preliminary Experiment Result	55
4.2.1	Different Welding Mode	55
4.2.2	Different Shielding Gas	56
4.2.3	Different Angle of Irradiation (AOI)	58
4.2.4	Fillet Lap Joint of Thin Sheet AZ31B	59
4.3	Tensile-Shear Strength	60
4.4	Macrostructure Analysis on Weld Appearance	62
4.4.1	Bond Width, Throat Length and Penetration Depth	64
4.5	Microstructure Analysis	68
4.6	Mathematical Modelling	71
4.7	Model Validation	73
4.8	Effects of Parameters on Tensile-shear Strength	75
4.9	Parameters Optimization	78
4.10	SEM and EDX analysis	80

4.10.1 Fracture Surface Morphology	80
4.10.2 Microstructure Evaluation	85
4.11 Micro-hardness	92
4.12 Defects	94
4.12.1 Cracks	94
4.12.2 Voids at root	95
4.13 Summary of Microstructure Evaluation	96
CHAPTER 5 CONCLUSION AND RECOMMENDATIONS	98
5.1 Introduction	98
5.2 Summary	98
5.3 Conclusion	101
5.4 Recommendations for Future Works	102
REFERENCES	103
LIST OF PUBLICATIONS	114
APPENDIX A	116
APPENDIX B	117

LIST OF TABLES

Table 2.1	Properties and typical forms of selected wrought magnesium alloys	10
Table 2.2	Properties of Magnesium, Aluminium, and iron at their melting point	10
Table 2.3	Summary for chemical composition of AZ31B	12
Table 2.4	Process variables and design level used in Box-Bhenken design	36
Table 2.5	Design matrix for three-level factors design with three centre points	37
Table 2.6	Analysis of variance table for the least squares fit of a model that is linear in its parameters	38
Table 2.7	Type of laser used to weld magnesium alloys	42
Table 3.1	Chemical composition of AZ31B	45
Table 3.2	Design matrix for three independent process factors	49
Table 4.1	Pre-experiment parameter for different welding mode	55
Table 4.2	Range of selected parameters	60
Table 4.3	Tensile shear strength result according to the experiment order	60
Table 4.4	Bond width, throat length, and penetration	65
Table 4.5	ANOVA for quadratic models	72
Table 4.6	ANOVA for reduced quadratic models	72
Table 4.7	Actual, predicted shear strength, and percentage error	73
Table 4.8	Optimized parameter with actual and predicted response	80
Table 4.9	Element percentage summary from EDX result of sample 1	82
Table 4.10	Element percentage summary from EDX result of optimized sample	84
Table 4.11	Microhardness values at different region	92

LIST OF FIGURES

Figure 2.1	Magnesium inner frame for LG smartphone	9
Figure 2.2	Micographs of AZ31B base metal using (a) OM and (b) SEM	9
Figure 2.3	Al-Mg binary phase diagram	11
Figure 2.4	Schematic illustration of laser element	13
Figure 2.5	Three stages to the laser generation	13
Figure 2.6	Remote laser welding in automotive application	14
Figure 2.7	Details of Gillette razor blades cartridge spot welded	15
Figure 2.8	Fiber laser with flexible glass fiber	16
Figure 2.9	A schematic of single and multimode fiber lasers.	16
Figure 2.10	Comparative study between (a) most popular lasers in industry and (b) operating cost for lasers in industries for 8 years period	18
Figure 2.11	Power versus time for CW mode	19
Figure 2.12	Penetration depth versus power density for an interaction time of 20 ms and a beam diameter of 0.95mm for the CW welds and a beam diameter of 0.9mm for the PW welds	20
Figure 2.13	Rectangular mode of pulse wave fiber laser	21
Figure 2.14	Characteristic lengths of welded spot as function of incident angle of laser beam	22
Figure 2.15	Tensile strength at room and high temperature between base metal, CW and PW joint of GH3535 superalloy	22
Figure 2.16	Two passes laser welding (a) defocused pre-heating (b) welding process	24
Figure 2.17	Rear diameter of the fusion bath vs. laser power for different pulse durations of 5 ms, 10 ms and 15 ms.	26
Figure 2.18	Weld appearances at different beam center locations and scan speed	27
Figure 2.19	Laser spot (a) top view and (b) cross section area	28
Figure 2.20	Laser spot with incident angle of 45 ° from (a) top view and (b) cross-sectioned sample	28
Figure 2.21	Setup for different laser beam incident angle	29
Figure 2.22	Surface appearances, X-ray inspection results and cross-sections of A5083 weld bead produced by 10kW fibre laser at various incident angles.	30
Figure 2.23	Microstructure of fusion zone of LBWed AZ31B with the XRD result	31
Figure 2.24	Optical microstructure of TIG welded AZ31B without flux	31
Figure 2.25	SEM/EDX in Fusion Zone of TIG welded AZ31B	32

Figure 2.26	Process factors and responses	33
Figure 2.27	Response surface with (a) no curvature (b) curvature	35
Figure 2.28	Central composite designs for two and three factors. The gray dots form the cubic part, the runs of the 22 and 23 factorial. The black dots represent the starparts.	35
Figure 2.29	Three factor of Box-Behnken design	36
Figure 2.30	Ideal line plotted between actual and predicted value	40
Figure 2.31	Optimization step for Box-Behnken design	41
Figure 3.1	Methodology flowchart	44
Figure 3.2	Sample dimension for Bead-on-Plate (BOP) welding	45
Figure 3.3	Sample dimension for double fillet lap joint	46
Figure 3.4	Low power fiber laser welding machine	46
Figure 3.5	Side view of welding condition	47
Figure 3.6	Front view of welding condition on filler lap joint of thin sheet AZ31B (a) schematic illustration and (b) front image	47
Figure 3.7	Tensile-shear sample (a) schematic image (b) tested sample	50
Figure 3.8	Schematic illustration of macrostructure evaluation	51
Figure 3.9	Average grain structure measurement	52
Figure 3.10	Vicker's hardness test (a) schematic illustration (b) position of indenter	52
Figure 4.1	Cross section images of BOP welded AZ31B for CW and PW mode	56
Figure 4.2	BOP welded of AZ31B with (a) Argon (b) Nitrogen (c) maximize image of part (a)	57
Figure 4.3	Schematic illustration for measurement of weld and underfill depth	58
Figure 4.4	Cross-section of BOP welded by AOI (a) 1° (b) 2° (c) 3° (d) 4° (e) 5°	58
Figure 4.5	Cross section image of fillet welded AZ31B (a) 2.0 J (b) 2.4 J	59
Figure 4.6	Fracture load and shear strength of fifteen welded samples	61
Figure 4.7	Macrostructure images of laser welded thin sheets AZ31B	63
Figure 4.8	Macrostructure images of (a) sample 1 and (b) sample 9	64
Figure 4.9	Fracture load (N) versus bond width (μm) at different pulsed energy	66
Figure 4.10	Fracture load (N) versus throat length (μm) at different pulsed energy	66
Figure 4.11	Fracture load (N) versus penetration depth (μm) at different pulsed energy	67
Figure 4.12	Microstructure images of sample 1 (a) top surface appearance (b) weld cross-section (c) FZ (d) centre of FZ (e) transition region (f) base metal	69

Figure 4.13	Microstructure images of sample 9 (a) top surface appearance (b) weld cross-section (c) FZ (d) centre of FZ (e) transition region (f) base metal	70
Figure 4.14	Normal distribution plot for standard residuals of the model	74
Figure 4.15	Scatter diagram of actual versus predicted responses	75
Figure 4.16	Main effect plot (MEP) for tensile shear strength	76
Figure 4.17	Contour plots of three responses for tensile shear strength	77
Figure 4.18	Surface plots of three responses for tensile shear strength at (a) hold value of AOI 3° (b) hold value of WS 3 mm/s,	77
Figure 4.19	Surface plots of three responses for tensile shear strength at hold value of EP 2 J	78
Figure 4.20	Optimization graph for minimum, target, and high response values	79
Figure 4.21	Fracture Surface Morphology of sample 1 (a) macrograph (b) SEM image of selected area from (a) (c) 1000 × magnification from area in (b) and EDX spectrums (d) 2000 × magnification from area in (c)	81
Figure 4.22	EDX results of spectrum 1, 2, and 3 for sample 1	82
Figure 4.23	Fracture surface morphology of optimized sample (a) macrograph (b) SEM image of selected area from (a) (c) 1000 × magnification from area in b and EDX spectrums (d) 1000 × magnification from area in (c) (e) 2000 × magnification from area in (d)	83
Figure 4.24	EDX results of spectrum 1, 2 and 3 for optimized sample	84
Figure 4.25	SEM image and EDX area scan of AZ31B base metal	85
Figure 4.26	SEM images of microstructure from welded cross section of sample 9	87
Figure 4.27	EDX analysis for sample 9	88
Figure 4.28	SEM images of microstructure at the first weld cross section of sample optimized	89
Figure 4.29	EDX analysis for sample optimized	91
Figure 4.30	Hardness test position for (a) sample 9 and (b) optimized sample	93
Figure 4.31	Comparison of hardness result for sample 9 and optimized sample at the weld cross section	93
Figure 4.32	Centre crack at sample 2 (a) top surface (b) cross section	94
Figure 4.33	Initiation of crack from the root to the centre of the weld from sample 11	94
Figure 4.34	Sample 7 with void at the weld root sample 8 with excess penetration and void at weld root	95

LIST OF SYMBOLS

γ	Shear strength
\approx	Approximately
$^{\circ}$	Degree
$^{\circ}\text{C}$	Degree Celsius
μ	Micro
$<$	Less than
$>$	More than
$\%$	Percentage
μm	Micro meter
μs	Micro seconds
$1/\text{K}$	Coefficient of thermal expansion
α	Alpha
β	Beta
b_0	Constant coefficient of regression
b_i, b_{ii}, b_{ij}	Coefficient regression
eV	Ionization energy
Σ	Summation
ft	Feet
HV	Vickers Hardness
J/mm	Joules per millimetre
$\text{J kg}^{-1}\text{K}^{-1}$	Specific heat
J/kg	Specific heat of fusion
kW	Kilo Watt
Kg m^{-3}	Density
$\text{Kg m}^{-1}\text{K}^{-1}$	Viscosity
mm	Millimetre
m^2S^{-1}	Thermal diffusivity
MPa	Mega Pascal
N	Newton
N m^{-1}	Surface tension
N/m^3	Elastic modulus
W	Watt
$\text{W m}^{-1}\text{K}^{-1}$	Thermal conductivity
x_i, x_{ii}, x_{ij}	Factors

LIST OF ABBREVIATIONS

Al	Aluminium
Ar	Argon
AOI	Angle of Irradiation
ANOVA	Analysis of Variance
BL	Bead Length
BM	Base Metal
BW	Bead Width
BBD	Box-Behnken Design
BOP	Bead on Plate
CW	Continuous Wave
CCD	Central Composite Design
CO ₂	Carbon Dioxide
DOE	Design of Experiment
EP	Pulsed Energy
EBW	Electron beam welding
EDX	Electron dispersive X-ray
FZ	Fusion Zone
FFD	Full Factorial Design
HV	Vickers Hardness
HAZ	Heat Affected Zone
HCP	Hexagonally Closely Packed
IMC	Intermetallic compound
LBW	Laser beam welding
LOF	Lack of fit
Mg	Magnesium
MIG	Metal inert gas
Nd:YAG	Neodymium: Ytterbium-Aluminium Garnet
O ₂	Oxygen
OM	Optical microscope
OFAT	One factor at a time
PD	Penetration depth
PW	Pulse Wave
PMZ	Partially melted zone
QCW	Quasi-continuous wave
RSM	Response Surface Method
SEM	Scanning electron microscope
TIG	Tungsten inert gas
VIF	Value of inflation
WS	Welding Speed
Zn	Zinc

REFERENCES

- Al-Kazzaz, H., Cao, X., Jahazi, M., and Medraj, M. (2008). Reliability of Laser Welding Process for ZE41A-T5 Magnesium Alloy Sand Castings. *Materials Transactions*, 49(4), pp.774-781.
- Anawa, E. M., and Olabi, A. G. (2008). Using Taguchi method to optimize welding pool of dissimilar laser-welded components. *Optics & Laser Technology*, 40(2), pp.379-388.
- Arif Demir, E. A., Timur Canel, Sarp Ertürk, Ali Arslan Kaya. (2007). Optimization of Nd:YAG Laser Welding of Magnesium. *Journal of Laser Micro/Nanoengineering*, 2, pp.108-113.
- Assunção, E., Quintino, L., and Miranda, R. (2009). Comparative study of laser welding in tailor blanks for the automotive industry. *The International Journal of Advanced Manufacturing Technology*, 49(1-4), pp.123-131.
- Assuncao, E., and Williams, S. (2013). Comparison of continuous wave and pulsed wave laser welding effects. *Optics and Lasers in Engineering*, 51(6), pp.674-680.
- Benyounis, K. Y., Olabi, A. G., and Hashmi, M. S. J. (2005a). Effect of laser welding parameters on the heat input and weld-bead profile. *Journal of Materials Processing Technology*, 164-165, pp.978-985.
- Benyounis, K. Y., Olabi, A. G., and Hashmi, M. S. J. (2005b). Optimizing the laser-welded butt joints of medium carbon steel using RSM. *Journal of Materials Processing Technology*, 164-165, pp.986-989.
- Brandizzi, M., Renna, S., Satriano, A., Sorgente, D., and Tricarico, L. (2013). Nd:YAG laser welding of fine sheet metal butt joints in AZ31 magnesium alloy. *Welding International*, 28(10), pp.784-792.
- Cao, X., Jahazi, M., Immarigeon, J. P., and Wallace, W. (2006). A review of laser welding techniques for magnesium alloys. *Journal of Materials Processing Technology*, 171(2), pp.188-204.

- Casalino, G., Guglielmi, P., Lorusso, V. D., Mortello, M., Peyre, P., and Sorgente, D. (2017). Laser offset welding of AZ31B magnesium alloy to 316 stainless steel. *Journal of Materials Processing Technology*, 242, pp.49-59.
- Cavazzuti, M. (2013). Design of Experiments *Optimization Methods: From Theory to Scientific Design and Technological Aspects in Mechanics* (pp. 13-42): Springer.
- Chi, C. T., and Chao, C. G. (2007). Characterization on electron beam welds and parameters for AZ31B-F extrusive plates. *Journal of Materials Processing Technology*, 182(1-3), pp.369-373.
- Coelho, R. S., Kostka, A., Pinto, H., Riekehr, S., Koçak, M., and Pyzalla, A. R. (2008). Microstructure and mechanical properties of magnesium alloy AZ31B laser beam welds. *Materials Science and Engineering: A*, 485(1-2), pp.20-30.
- Cui, Z. Q., Shi, H. X., Wang, W. X., and Xu, B. S. (2015). Laser surface melting AZ31B magnesium alloy with liquid nitrogen-assisted cooling. *Transactions of Nonferrous Metals Society of China*, 25(5), pp.1446-1453.
- Divya Deep Dhancholia, Anuj Sharma, and Vyas, C. (2014). Optimisation of Friction Stir Welding Parameters for AA 6061 and AA 7039 Aluminium Alloys by Response Surface Methodology (RSM). *International Journal of Advanced Mechanical Engineering*, 4, pp.565-571.
- Esraa, K. H., Farah, H., and Makram, F. (2014). Laser wavelength and energy effect on optical and structure properties for nano titanium oxide prepared by pulsed laser deposition. *Iraqi Journal of Physics*, 12(25), pp.62-68.
- Falconnet, E., Chambert, J., Makich, H., and Monteil, G. (2015). Prediction of abrasive punch wear in copper alloy thin sheet blanking. *Wear*, 338-339, pp.144-154.
- Ferreira, S. L., Bruns, R. E., da Silva, E. G., Dos Santos, W. N., Quintella, C. M., David, J. M., de Andrade, J. B., Breikreitz, M. C., Jardim, I. C., and Neto, B. B. (2007). Statistical designs and response surface techniques for the optimization of chromatographic systems. *J Chromatogr A*, 1158(1-2), pp.2-14.

- Fleming, S. 2012. *An Overview of Magnesium based Alloys for Aerospace and Automotive Application*. Master Of Engineering In Mechanical Engineering. Rensselaer Polytechnic Institute, Faculty of Rensselaer Polytechnic Institute
- Florin. (2010). All LG mobile phones to utilize Eco-Magnesium by 2012. Available at: <http://www.unwiredview.com/2010/12/06/all-lg-phones-to-utilize-eco-magnesium-by-2012/>. (Accessed on 17 June)
- Forcellese, A., Gabrielli, F., and Simoncini, M. (2012). Mechanical properties and microstructure of joints in AZ31 thin sheets obtained by friction stir welding using “pin” and “pinless” tool configurations. *Materials & Design*, 34, pp.219-229.
- Fuerschbach, P. W., and Eisler, G. R. (2002). Effect of laser spot weld energy and duration on melting and absorption. *Science and Technology of Welding and Joining*, 7(4), pp.241-246.
- Gisario, A., Veniali, F., Barletta, M., Tagliaferri, V., and Vesco, S. (2017). Laser transmission welding of poly(ethylene terephthalate) and biodegradable poly(ethylene terephthalate) – Based blends. *Optics and Lasers in Engineering*, 90, pp.110-118.
- Grupp, M., Klinker, K., and Cattaneo, S. (2013). Welding of high thicknesses using a fibre optic laser up to 30 kW. *Welding International*, 27(2), pp.109-112.
- Guan, Y. C., Zhou, W., Zheng, H. Y., and Li, Z. L. (2013). Darkening effect on AZ31B magnesium alloy surface induced by nanosecond pulse Nd:YAG laser. *Applied Surface Science*, 280, pp.462-466.
- Harooni, M. (2012). Studying the Effect of Laser Welding Parameters on the Quality of ZEK100 Magnesium Alloy Sheets in Lap Joint Configuration (pp. 11). Center for Laser-aided Manufacturing, Lyle School of Engineering: Southern Methodist University.
- Harooni, M., Carlson, B., and Kovacevic, R. (2014). Detection of defects in laser welding of AZ31B magnesium alloy in zero-gap lap joint configuration by a real-time spectroscopic analysis. *Optics and Lasers in Engineering*, 56, pp.54-66.

- Harooni, M., Ma, J., Carlson, B., and Kovacevic, R. (2015). Two-pass laser welding of AZ31B magnesium alloy. *Journal of Materials Processing Technology*, 216, pp.114-122.
- Hiraga, H., Inoue, T., Kamado, S., and Kojima, Y. (2002). Effects of the shielding gas and laser wavelength in laser welding magnesium alloy sheets. *Welding International*, 16(6), pp.442-450.
- Huang, H., Wang, J., Li, L., and Ma, N. (2016). Prediction of laser welding induced deformation in thin sheets by efficient numerical modeling. *Journal of Materials Processing Technology*, 227, pp.117-128.
- Ishak, M., Islam, M. R., and Sawa, T. (2014). GMA Spot Welding of A7075-T651/AZ31B Dissimilar Alloys Using Stainless Steel Filler. *Materials and Manufacturing Processes*, 29(8), pp.980-987.
- Ishak, M., Maekawa, K., and Yamasaki, K. (2012). The characteristics of laser welded magnesium alloy using silver nanoparticles as insert material. *Materials Science and Engineering: A*, 536, pp.143-151.
- Ishak, M., Yamasaki, K., and Maekawa, K. (2009). Lap Fillet Welding of Thin Sheet AZ31 Magnesium Alloy with Pulsed Nd:YAG Laser. *Journal of Solid Mechanics and Materials Engineering*, 3(9), pp.1045-1056.
- Ishak, M., Yamasaki, K., and Maekawa, K. (2010). Lap Fillet Laser Welding of AZ31B Thin Sheet Magnesium Alloy using Silver Nanoparticles. *Journal of Solid Mechanics and Materials Engineering*, 4(1), pp.51-62.
- Ishak, M., Yamasaki, K., and Maekawa, K. (2012). Laser Welding of Thin Sheet Magnesium Alloys. In I. Tech (Ed.), *Nd:YAG Lasers* (Vol. 2016, pp. 135-157): In Tech Open Access.
- Jiang, M. Q., Wu, X. Q., Wei, Y. P., Wilde, G., and Dai, L. H. (2017). Cavitation bubble dynamics during pulsed laser ablation of a metallic glass in water. *Extreme Mechanics Letters*, 11, pp.24-29.

- Jiang, Z., Tao, W., Yu, K., Tan, C., Chen, Y., Li, L., and Li, Z. (2016). Comparative study on fiber laser welding of GH3535 superalloy in continuous and pulsed waves. *Materials & Design*, 110, pp.728-739.
- Jing, W., Hui, C., Qiong, W., Hongbo, L., and Zhanjun, L. (2017). Surface modification of carbon fibers and the selective laser sintering of modified carbon fiber/nylon 12 composite powder. *Materials & Design*, 116, pp.253-260.
- Joost, W. J., and Krajewski, P. E. (2017). Towards magnesium alloys for high-volume automotive applications. *Scripta Materialia*, 128, pp.107-112.
- Juan Hu, L., Peng, Y. H., Yong Li, D., and Rui Zhang, S. (2010). Influence of Dynamic Recrystallization on Tensile Properties of AZ31B Magnesium Alloy Sheet. *Materials and Manufacturing Processes*, 25(8), pp.880-887.
- Kalpakjian, S., and Schmid, S. R. (2010a). Laser Beam Welding *Manufacturing Engineering and Technology* (6 ed., pp. 880-881): Prentice Hall.
- Kalpakjian, S., and Schmid, S. R. (2010b). Magnesium and Magnesium Alloys *Manufacturing Engineering and Technology* (sixth ed., pp. 157-158): Prentice Hall.
- Kansal, H. K., Singh, S., and Kumar, P. (2005). Parametric optimization of powder mixed electrical discharge machining by response surface methodology. *Journal of Materials Processing Technology*, 169(3), pp.427-436.
- Karen. (2016). Assessing the Fit of Regression Models. Available at: <http://www.theanalysisfactor.com/assessing-the-fit-of-regression-models/>. (Accessed on March 15)
- Katayama, S., Nagayama, H., Mizutani, M., and Kawahito, Y. (2009). Fibre laser welding of aluminium alloy. *Welding International*, 23(10), pp.744-752.
- Katayama, S., and Ogawa, K. (2013). Laser weldability and ageing characteristics of welds: laser weldability of commercially available A7N01 alloy (1). *Welding International*, 27(3), pp.172-183.

- Katayama Seiji, A. Y., Mizutani Masami, Kawahito Yousuke. (2011). Deep Penetration Welding with High-Power Laser under Vacuum. *Transactions of JWRI*, 40(1), pp.5.
- Kawahito, Y., Matsumoto, N., Abe, Y., and Katayama, S. (2012). Laser absorption of aluminium alloy in high brightness and high power fibre laser welding. *Welding International*, 26(4), pp.275-281.
- Kenji, O., and Masatoshi, M. (2015). Recent Trend of Welding Technology Development and Applications *JFE Technical Report* (pp. 8). Chiyodaku, Tokyo, Japan: JFE Holdings, Inc.
- Kumar, N., Mukherjee, M., and Bandyopadhyay, A. (2017). Study on laser welding of austenitic stainless steel by varying incident angle of pulsed laser beam. *Optics & Laser Technology*, 94, pp.296-309.
- Leong, K. H. (1999). Laser beam welding of AZ31B-H24 magnesium alloy. <http://digital.library.unt.edu/ark:/67531/metadc623699/>
- Levin, Y. Y., and Erofeev, V. A. (2009). Calculation of the parameters of pulsed laser welding of thin sheets of aluminium alloys. *Welding International*, 23(12), pp.934-938.
- Li, W., Zhao, G., Ma, X., and Gao, J. (2013). Study on Forming Limit Diagrams of AZ31B Alloy Sheet at Different Temperatures. *Materials and Manufacturing Processes*, 28(3), pp.306-311.
- Li, Y., Huang, J., Cui, H., and Zhang, J. (2008). Characterization of microstructure evolution and mechanical properties of the spray-deposited AZ31 magnesium alloy. *Journal of University of Science and Technology Beijing Mineral Metallurgy Material*, 6(15), pp.740-746.
- Liao, Y. C., and Yu, M. H. (2007). Effects of laser beam energy and incident angle on the pulse laser welding of stainless steel thin sheet. *Journal of Materials Processing Technology*, 190(1-3), pp.102-108.

- Lin, C. M., Liu, J. J., Tsai, H. L., and Cheng, C. M. (2011). Evolution of microstructures and mechanical properties of AZ31B magnesium alloy weldment with active oxide fluxes and GTAW process. *Journal of the Chinese Institute of Engineers*, 34(8), pp.1013-1023.
- Lin, R., Wang, H., Lu, F., Solomon, J., and Carlson, B. E. (2017). Numerical study of keyhole dynamics and keyhole-induced porosity formation in remote laser welding of Al alloys. *International Journal of Heat and Mass Transfer*, 108, pp.244-256.
- Litron. (2015). CW Welding vs Pulse Welding. Available at: <http://www.litron.com/wp/cw-welding-vs-pulse-welding/>. (Accessed on 10 January)
- Liu, L., and Hao, X. (2010). Low-Power Laser/TIG Hybrid Welding Process of Magnesium Alloy with Filler Wire. *Materials and Manufacturing Processes*, 25(11), pp.1213-1218.
- Liu, L., Ren, D., and Liu, F. (2014). A Review of Dissimilar Welding Techniques for Magnesium Alloys to Aluminum Alloys. *Materials*, 7(5), pp.3735-3757.
- Ma, J., Harooni, M., Carlson, B., and Kovacevic, R. (2014). Dissimilar joining of galvanized high-strength steel to aluminum alloy in a zero-gap lap joint configuration by two-pass laser welding. *Materials & Design*, 58, pp.390-401.
- Manohar, M., Joseph, J., Selvaraj, T., and Sivakumar, D. (2013). Application of Box Behnken Design to Optimize the Parameters for Turning Inconel 718 using Coated Carbide Tools. *International Journal of Scientific & Engineering Research*, 4(4), pp.23.
- Margaret, R. (2016). Definition Laser. Available at <http://whatis.techtarget.com/definition/laser>. (Accessed on 10 October)
- Mei, L., Yan, D., Chen, G., Wang, Z., and Chen, S. (2017). Influence of laser beam incidence angle on laser lap welding quality of galvanized steels. *Optics Communications*, 402, pp.147-158.
- Michael, D. L., and Shin, H. S. (2017). Weldability assessment of Mg alloy (AZ31B) sheets by an ultrasonic spot welding method. *Journal of Materials Processing Technology*, 243, pp.1-8.

- Minitab. (2017a). What is a Box-Behnken design? Available at:<http://support.minitab.com/en-us/minitab/17/topic-library/modeling-statistics/doe/response-surface-designs/what-is-a-box-behnken-design/>. (Accessed on 15 January)
- Minitab. (2017b). What is a response surface design? Available at: <http://support.minitab.com/en-us/minitab/17/topic-library/modeling-statistics/doe/response-surface-designs/what-is-a-response-surface-design/>. (Accessed on 15 January)
- Mishra, S., Sridhara, N., Mitra, A., Yougandar, B., Dash, S. K., Agarwal, S., and Dey, A. (2017). CO₂ laser cutting of ultra thin (75µm) glass based rigid optical solar reflector (OSR) for spacecraft application. *Optics and Lasers in Engineering*, 90, pp.128-138.
- Miyachi, A. (2015). Laser Welding Fundamentals. Available at:http://www.amadamiyachi.com/servlet/servlet.FileDownload?retURL=%2Fapex%2Feducationalresources_articles&file=01580000001Jz8A. (Accessed on 5 February)
- Molnár, P., Ostapovets, A., and Jäger, A. (2014). Reversible motion of twin boundaries in AZ31 alloy and new design of magnesium alloys as smart materials. *Materials & Design*, 56, pp.509-516.
- Monteiro, W. A. (2014). The Influence of Alloy Element on Magnesium for Electronic Devices Applications – A Review *Light Metal Alloys Applications: InTech*.
- Moskvitin, G. V., Polyakov, A. N., and Birger, E. M. (2013). Application of laser welding methods in industrial production. *Welding International*, 27(7), pp.572-580.
- Newport. (2016). Average and Peak Power-A Tutorial. Available at:<http://hank.uoregon.edu/experiments/modelocked-fiberlaser/20063.pdf>. (Accessed on 10 May)
- Ngoc, T. N., Oh, S. S., Chung, A. L., Myoung, G. L., Ji, h. K., and Heon, Y. K. (2014). Mechanical Behavior of AZ31B Mg Alloy Sheets under Monotonic and Cyclic Loadings at Room and Moderately Elevated Temperatures. *Materials*, 7, pp.24.
- Odabaşı, A., Ünlü, N., Göller, G., and Eruslu, M. N. (2010). A Study on Laser Beam Welding (LBW) Technique: Effect of Heat Input on the Microstructural Evolution of Superalloy Inconel 718. *Metallurgical and Materials Transactions A*, 41(9), pp.2357-2365.

- Padmanaban, G., and Balasubramanian, V. (2010). Optimization of laser beam welding process parameters to attain maximum tensile strength in AZ31B magnesium alloy. *Optics & Laser Technology*, 42(8), pp.1253-1260.
- Padmanaban, G., and Balasubramanian, V. (2011). Effects of laser beam welding parameters on mechanical properties and microstructure of AZ31B magnesium alloy. *Transactions of Nonferrous Metals Society of China*, 21(9), pp.1917-1924.
- Pan, F., Zeng, B., Jiang, B., Zhang, M., and Dong, H. (2017). Enhanced mechanical properties of AZ31B magnesium alloy thin sheets processed by on-line heating rolling. *Journal of Alloys and Compounds*, 693, pp.414-420.
- Pan, H., Ren, Y., Fu, H., Zhao, H., Wang, L., Meng, X., and Qin, G. (2016). Recent developments in rare-earth free wrought magnesium alloys having high strength: A review. *Journal of Alloys and Compounds*, 663, pp.321-331.
- Pocorni, J., Powell, J., Deichsel, E., Frostevarg, J., and Kaplan, A. F. H. (2016). Fibre laser cutting stainless steel: Fluid dynamics and cut front morphology. *Optics & Laser Technology*, 87, pp.87-93.
- Reimann, W., Pfriem, S., Hammer, T., Pätke, D., Ungers, M., and Dilger, K. (2017). Influence of different zinc coatings on laser brazing of galvanized steel. *Journal of Materials Processing Technology*, 239, pp.75-82.
- Rolink, G., Weisheit, A., Biermann, T., Bobzin, K., Öte, M., Linke, T. F., Schulz, C., and Kelbassa, I. (2014). Investigations of laser clad, thermal sprayed and laser remelted AlSi20-coatings on magnesium alloy AZ31B under constant and cycling thermal load. *Surface and Coatings Technology*, 259, pp.751-758.
- Ross, P. J. (1996). *Taguchi techniques for quality engineering*. New York: McGraw-Hill.
- Sanders, P. G., Keske, J. S., Leong, K. H., and Kornecki, G. (1999). High power Nd:YAG and CO₂ laser welding of magnesium. *Journal Laser Applications*, 11(96).
- Schweier, M., Haubold, M. W., and Zaeh, M. F. (2016). Analysis of spatters in laser welding with beam oscillation: A machine vision approach. *CIRP Journal of Manufacturing Science and Technology*, 14, pp.35-42.

- Shannon, G. (2017). Choosing between Nd:YAG or fiber lasers for micro welding. Available at: <http://www.industrial-lasers.com/articles/2016/10/choosing-between-nd-yag-or-fiber-lasers-for-micro-welding.html>. (Accessed on 10 January)
- Simoncini, M., and Forcellese, A. (2012). Effect of the welding parameters and tool configuration on micro- and macro-mechanical properties of similar and dissimilar FSWed joints in AA5754 and AZ31 thin sheets. *Materials & Design*, 41, pp.50-60.
- Sivaros, Milkey, K. R., Samsudin, A. R., Dubey, A. K., and Kidd, P. (2014). Comparison between Taguchi Method and Response Surface Methodology (RSM) in Modelling CO2 Laser Machining. *Jordan Journal of Mechanical and Industrial Engineering*, 8(1), pp.35-42.
- Steglich, D., Tian, X., Bohlen, J., and Kuwabara, T. (2014). Mechanical Testing of Thin Sheet Magnesium Alloys in Biaxial Tension and Uniaxial Compression. *Experimental Mechanics*, 54(7), pp.1247-1258.
- Subravel, V., Padmanaban, G., and Balasubramanian, V. (2014). Effect of welding speed on microstructural characteristics and tensile properties of GTA welded AZ31B magnesium alloy. *Transactions of Nonferrous Metals Society of China*, 24(9), pp.2776-2784.
- Sundarajan, K. (2017). Design of Experiments – A Primer. Available at: <https://www.isixsigma.com/tools-templates/design-of-experiments-doe/design-experiments-%E2%90%93-primer/>. (Accessed on 10 January)
- Tan, Q., Atrens, A., Mo, N., and Zhang, M.-X. (2016). Oxidation of magnesium alloys at elevated temperatures in air: A review. *Corrosion Science*, 112, pp.734-759.
- Tong, H., Ueyama, T., Kihara, T., Nakata, K., and Ushio, M. (2005). High speed welding of aluminium alloy sheets with using the laser/AC pulsed MIG hybrid process. *Welding International*, 19(2), pp.89-99.
- Torkamany, M. J., Malek Ghaini, F., Poursalehi, R., and Kaplan, A. F. H. (2016). Combination of laser keyhole and conduction welding: Dissimilar laser welding of niobium and Ti-6Al-4V. *Optics and Lasers in Engineering*, 79, pp.9-15.
- Tsuji, M. (2009). IPG fibre lasers and aluminium welding applications. *Welding International*, 23(10), pp.717-722.

- Tur, A., Cordovilla, F., García-Beltrán, Á., and Ocaña, J. L. (2017). Minimization of the thermal material effects on pulsed dynamic laser welding. *Journal of Materials Processing Technology*, 246, pp.13-21.
- Ventrella, V. A., Berretta, J. R., and de Rossi, W. (2011). Micro Welding of Ni-based Alloy Monel 400 Thin Foil by Pulsed Nd:YAG laser. *Physics Procedia*, 12, pp.347-354.
- Wahba, M., and Katayama, S. (2012). Laser welding of AZ31B magnesium alloy to Zn-coated steel. *Materials & Design*, 35, pp.701-706.
- Wahba, M., Mizutani, M., Kawahito, Y., and Katayama, S. (2012). Laser welding of die-cast AZ91D magnesium alloy. *Materials & Design*, 33, pp.569-576.
- Wu, H. Y., Sun, P. H., Zhu, F. J., Liu, H. C., and Chiu, C. H. (2012). Tensile Properties and Shallow Pan Rapid Gas Blow Forming of Commercial Fine-grained Mg Alloy AZ31B Thin Sheet. *Procedia Engineering*, 36, pp.329-334.
- Yan, H. G., Zhao, Q., Chen, P., Chen, J. H., and Su, B. (2015). Microstructures and mechanical properties of laser welded wrought fine-grained ZK60 magnesium alloy. *Transactions of Nonferrous Metals Society of China*, 25(2), pp.389-396.
- Yan, Y., Zhang, D. T., Qiu, C., and Zhang, W. (2010). Dissimilar friction stir welding between 5052 aluminum alloy and AZ31 magnesium alloy. *Transaction of Nonferrous Metal Society China*, 20, pp.619-623.
- Yu, Z. H., Yan, H. G., Yin, X. Y., Li, Y., and Yan, G. H. (2012). Liquation cracking in laser beam welded joint of ZK60 magnesium alloy. *Transactions of Nonferrous Metals Society of China*, 22(12), pp.2891-2897.
- Zhang, N., Wang, W., Cao, X., and Wu, J. (2015). The effect of annealing on the interface microstructure and mechanical characteristics of AZ31B/AA6061 composite plates fabricated by explosive welding. *Materials & Design (1980-2015)*, 65, pp.1100-1109.
- Zhao, Y., Ding, Z., Shen, C., and Chen, Y. (2016). Interfacial microstructure and properties of aluminum–magnesium AZ31B multi-pass friction stir processed composite plate. *Materials & Design*, 94, pp.240-252.